BMC Infectious Diseases

RESEARCH

Open Access

Bone features reinforce differential diagnosis between tuberculous spondylitis and brucellosis spondylitis

Qinpeng Xu[1†], Xingzhi Jing[1†], Meimei Zheng[2†], Jianmin Sun[1], Xingang Cui[1] and Xiaoyang Liu[1*]

Abstract

Background Tuberculous spondylitis (TS) and brucellar spondylitis (BS) both cause major long-term morbidity and disability. Though Spondylodiscitis is sensitive to magnetic resonance images, some are difficult to differentiate. This study aims to identify specific bone changes on computed tomography (CT) images, further to differentiate TS from BS.

Methods We retrospectively analyzed and enrolled 70 patients with TS and 65 with BS at our hospital from December 2012 to January 2024. Information of bone destruction and formation, vertebral wall integrity, osteosclerosis, and sequestrum on CT images was collected and compared using the chi-square test or *t*-test. $P<0.01$ was considered statistically significant.

Results Bone destruction was greater in the TS group compared to the BS group (519.55 mm^2 vs. 316.00 mm^2, $t=6.01$, $P<0.001$), preferentially involving each third of the vertebral body horizontally (41.22% vs. 16.67%, $\chi^2=77.76$, $P<0.001$; positive predictive value [PPV] = 80.6%) and the area under the endplate and equatorial portion of the vertebra longitudinally (80.53% vs. 28.20%, $\chi^2=134.19$, $P<0.001$, PPV = 82.75%). Patients with BS more frequently exhibited fan-shaped osteosclerosis (12.82% vs. 1.15%, $\chi^2=71.30$, $P<0.001$; PPV = 86.96%), longer bone formation surrounding the vertebra (18.06 mm vs. 1.97 mm, $t=14.28$, $P<0.001$), and longer anterior bone formation (3.86 mm vs. 0.92 mm, $t=6.51$, $P<0.001$). Anterior and closed bone formation was more common in the BS group than in the TS group (44.87% vs. 7.63%, $\chi^2=152.53$, $P<0.001$; PPV = 77.78%). Fragmented and blocked sequestrum was more common in the TS group than in the BS group and tended to spread in and out of the erosions (22.14% vs. 0.64%, PPV = 98.31% and 22.14% vs. 0.00%, PPV = 100%, $\chi^2=102.43$, $P<0.001$).

Conclusions TS and BS exhibit specific features of bone formation, bone destruction, and sequestrum on CT imaging. Our findings indicate that bone features on CT can help clinicians distinguish between two spinal infections.

Keywords CT images, Infection, Tuberculous spondylitis, Brucellosis spondylitis, Differential diagnosis

†Qinpeng Xu, Xingzhi Jing and Meimei Zheng contributed equally to this work.

*Correspondence:
Xiaoyang Liu
liuxiaoyang@sdfmu.edu.cn

[1]Department of Spine Surgery, Shandong Provincial Hospital Affiliated to Shandong First Medical University, 9677 Jingshi Road, Jinan 250021, China
[2]Department of Neurology, The First Affiliated Hospital of Shandong First Medical University & Shandong Provincial Qianfoshan Hospital, 16766 Jingshi Road, Jinan City, China

© The Author(s) 2024. **Open Access** This article is licensed under a Creative Commons Attribution-NonCommercial-NoDerivatives 4.0 International License, which permits any non-commercial use, sharing, distribution and reproduction in any medium or format, as long as you give appropriate credit to the original author(s) and the source, provide a link to the Creative Commons licence, and indicate if you modified the licensed material. You do not have permission under this licence to share adapted material derived from this article or parts of it. The images or other third party material in this article are included in the article's Creative Commons licence, unless indicated otherwise in a credit line to the material. If material is not included in the article's Creative Commons licence and your intended use is not permitted by statutory regulation or exceeds the permitted use, you will need to obtain permission directly from the copyright holder. To view a copy of this licence, visit http://creativecommons.org/licenses/by-nc-nd/4.0/.

Background

Tuberculosis (TB) is a leading cause of morbidity and mortality worldwide [1]. In 2017, there were an estimated 10 million incident TB cases and 1.6 million deaths from TB globally [2]. Tubercular spondylitis (TS) is the most common form of musculoskeletal TB and accounts for approximately 20% of cases [3]. Rates of long-term TS-related morbidity and disability are increasing, especially in developing countries [4].

Brucellosis, caused by the brucella bacterium, remains a major health problem in many parts of the world [5]. However, prompt diagnosis of brucellar spondylitis (BS) remains difficult because the clinical findings are nonspecific.

TS and BS are both common spinal infections and share several clinical manifestations (back pain, fever, and elevated inflammatory markers), which makes it difficult to distinguish between these entities [6]. Although biopsy and culture is the diagnostic gold standard for infectious diseases, it has the low positivity rates for both bacteria, which were reportedly less than 50% for TS [7] and approximately 32% for BS [8]. XpertMTB/RIF generally refers to the rapid detection of Mycobacterium tuberculosis and rifampicin resistance, which is commonly used in clinic for rapid diagnosis of tuberculosis. A next-generation Xpert MTB/RIF assay was reported to have better detection rates for mycobacterium in spinal specimens [9]. However, the diagnostic value of this assay is limited by the inconvenience of obtaining necessary biopsy specimens in patients with infections. Meanwhile, both methods are time-consuming and inconvenient, limiting the prompt diagnosis between TS and BS. Therefore, it is urgent to identify another method of early diagnosis.

With the rapid development and increasing popularity of imaging techniques, there is increasing interest in identification of specific radiological features of TS and BS [10–12]. Magnetic resonance imaging (MRI) is the preferred modality for the diagnosis and assessment of TS [13]. However, despite much research on spinal infections, no satisfactory strategy has been established for the differentiation of MRI in TS and BS.

Although MRI is sensitive to infectious spondylitis, it cannot clearly display changes in bone structure, which decrease the value of differential diagnosis between TS and BS. CT is preferred for the early diagnosis of pulmonary TB [14]. A previous report described CT imaging characteristics that help to differentiate pyogenic spondylitis from BS [15], identifying the value of bone changes in differentiating spinal infections. In this study, we sought to identify distinguishing features of TS and BS on CT images in order to help clinicians promptly differentiate these two spinal infections, further to improve cure rate, reduce recurrence rate, alleviate patient pain and decrease social economic burden.

Materials and methods

Patients

This retrospective study was approved by the Medical Ethics Committee of Shandong Provincial Hospital Affiliated to Shandong First Medical University (SZRJJ: NO.2022−136). Informed consent was obtained from all study participants. The study population was comprised of 248 consecutive patients from our hospital in eastern China from December 2012 to January 2024. 113 patients were excluded because of spinal pyogenic infection, postoperative infection, or incomplete course information. All study participants consented to conventional spinal CT examination before receiving treatment and were followed up until resolution of symptoms. The minimum follow-up duration was 6 months. The study finally enrolled 70 patients with TS and 65 with BS.

Diagnosis of TS was established by clinical, laboratory, imaging, and pathological examinations [12, 16] Pathological evidence of TB, including bacterial growth in biopsy specimens, caseating granulomatosis on histopathology, and the presence of acid-fast bacilli on Ziehl–Neelsen-stained slides, was considered the gold standard for diagnosis.

BS was diagnosed based on clinical symptoms and signs compatible with the disease (back pain, fever, sweats, fatigue, hepatosplenomegaly) and the presence of specific antibodies at significant titers (Standard Tube Agglutination [STA] test for brucella≥1/100) and/or isolation of brucella species in blood or biopsy specimens [17]. Other criteria included a duration of more than 1 year of STA testing for brucella≥1/50 and infection in the vertebra or intervertebral disc on MRI.

CT imaging

A 64-row MDCT scanner (mostly using the Somatom Sensation Cardiac, Siemens Healthineers; some using the Aquilion 64, Toshiba or LightSpeed 64, GE) was used for the radiological examinations. Parameters were set at 120 kVp or 140 kVp with a tube load of 180–310 mAs depending on patient weight and size. Coronal, sagittal, and axial reformations with a 2-mm section thickness were created from the primary source data with a 0.7 mm section thickness. The CT images were reviewed by two musculoskeletal radiologists blinded to the clinical data, each with more than 10 years of experience. Any disagreements were resolved according to the third radiologist.

Imaging evaluation

The anatomic vertebral and disc heights were measured on midsagittal images. The dimensions and locations of maximal erosion and bone formation were measured on sagittal images with maximal erosion and on axial images adjacent to the endplate cortex. Bone destruction was

categorized into 10 types in the same manner as our previous study [15]. Extensive destruction was defined as involvement of each third of the vertebral body horizontally. Longitudinal location of erosion was categorized into five types (none, endplate, area under the endplate, equatorial portion of vertebra, and both the area under the endplate and the equatorial portion of the vertebra). The rate of height loss was calculated as the height of the destroyed vertebra divided by the original vertebral height. The length and location of the destroyed vertebral wall were recorded on axial images. The length, width, and location of paraspinal bone formation were also assessed on both axial and sagittal images. Anterior bone formation was classified into five types (none, dotted, parallel, open, or closed) [15]. Axial location of sequestrum was divided into three types (none, in the erosions, in and out of the erosions). The morphological presentation of sequestrum was categorized as none, dotted, linear, fragmented, and blocked.

Statistical analysis

The normality of the data distribution was assessed using the Shapiro–Wilk test. Pearson's chi-square test was used for the categorical data. Continuous variables were compared using the independent samples *t*-test. Receiver-operating characteristic (ROC) curves were used to evaluate the diagnostic value and to select optimum cut-off values. The positive predictive values (PPVs) of specific imaging features for detection of TS or BS were calculated. All statistical analyses were performed using SPSS software (version 27; IBM Corp., Armonk, NY, USA). A two-sided *P*-value < 0.01 was considered statistically significant.

Table 1 Detailed information of patients' demographic and clinical characteristics

	TS group	BS group
No. of patient	70	65
Male	33	42
Female	37	23
Age	56(15–72)	57(25–74)
Fever	25	33
Back pain	61	62
Neurological deficiency	9	3
Level of involvement		
Cervical spine	9	4
Thoracic spine	77	27
Thoracolumbar spine	23	31
Lumbar spine	76	75
No. of involved vertebrae	185	137
Mean No. of involved vertebrae	2.64	2.11
The duration of symptoms before presentation (month)	3.85	5.36

Results

Seventy patients with TS (33 men, 37 women; mean age 56 [range, 15–72] years) and 65 with BS (42 men, 23 women; mean age 57 [range,25–74] years) were included in the study. Detailed information on patient demographics and clinical characteristics is provided in Table 1. No significant difference was found in the sex distribution and age at onset. The mean interval between presentation and CT imaging was 7.37 and 4.36 months in the TS and PS group, respectively, which was not statistically different. There was no statistical difference for the mean duration between presentation and confirmed diagnosis between the two groups. Most patients were cured through drug therapy. Nine patients from the TS group and Three patients from the BS group accepted decompression and internal fixation procedure because of neurological deficit or deformity.

The TS group included cervical ($n=5$), thoracic ($n=19$), thoracolumbar ($n=15$), and lumbar ($n=31$) cases. A total of 185 vertebrae were infected, and the mean number of involved vertebrae was 2.64 per patient. More than four vertebrae were involved in three patients, one of whom had involvement of nine vertebrae.

The BS group consisted of cervical ($n=2$), thoracic ($n=10$), thoracolumbar ($n=18$), and lumbar ($n=35$) cases. The lumbar spine was the site most commonly infected. 137 vertebrae were infected. The average number of destroyed vertebrae was 2.11 per patient. No patient had involvement of more than four vertebrae.

Information on bone destruction and its diagnostic significance is provided in Table 2. The sagittal and coronal diameters of erosion were significantly greater in the TS group than in the BS group (17.38 mm vs. 13.69 mm, $P<0.001$ and 21.12 mm vs. 15.69 mm, $P<0.001$, respectively); similarly, the area destroyed and the destruction rate were greater in the TS group (519.55mm^2 vs. 316.00mm^2, $P<0.001$ and 44.44% vs. 19.92%, $P<0.001$). The PPV of a destruction rate of more than 0.32 for detection of TS was 85.28%. Different morphologies of bone destruction on axial images were observed between the two groups (Fig. 1). Extensive destruction was more common in the TS group than in the BS group (41.22% vs. 16.67%, $\chi^2=77.76$, $P<0.001$) with a PPV for detection of TS of 80.6% (Fig. 2a). The posterior elements (pedicle, lamina, facet, transverse process, and spinous process) and peripheral bone (vertebral body except in the center and in the vertebral wall) were destroyed more often in the BS group (Fig. 2c). The rate of vertebral height loss was greater in the TS group (51.61% vs. 26.78%, $P<0.001$) with a PPV of more than 0.44 for detecting TS in 91.03% of cases. Erosions in the TS group commonly involved the area under the endplate and equatorial portion of the vertebra (Fig. 2b), whereas the endplate and area under the endplate were more easily destroyed in the BS group

Table 2 Bone destruction and its diagnostic significance

	Tuberculous Spondylitis	Brucellar Spondylitis	t-test	*P* value	Area Under Curve	Cut-off	Positive Predictive Value
Sagittal vertebral diameter (mm)							
Intrinsic (mm)	30.83 ± 6.89	34.80 ± 5.29					
Destructed (mm)	17.38 ± 8.98	13.69 ± 8.06	4.33	<0.001	0.62	17.18	0.74
Rate	0.57 ± 0.27	0.40 ± 0.23	6.64	<0.001	0.68	0.49	0.76
Area of vertebra (mm)							
Intrinsic (mm)	1182.36 ± 473.19	1615.19 ± 411.51					
Destructed (mm)	519.55 ± 401.98	316.00 ± 287.54	6.01	<0.001	0.66	414.90	0.78
Rate	0.44 ± 0.28	0.20 ± 0.16	11.27	<0.001	0.76	0.32	0.85
Hight of vertebra (mm)							
Intrinsic (mm)	17.26 ± 7.98	24.62 ± 8.51					
Destructed (mm)	9.30 ± 4.97	6.57 ± 4.31	5.91	<0.001	0.67	9.68	0.82
Rate	0.52 ± 0.16	0.27 ± 0.16	15.13	<0.001	0.86	0.44	0.91
Length of vertebra wall (mm)							
Intrinsic (mm)	124.52 ± 45.61	144.07 ± 19.70					
Destructed (mm)	54.85 ± 37.60	33.53 ± 27.83	6.62	<0.001	0.66	55.19	0.83
Rate	0.47 ± 0.41	0.23 ± 0.19	8.14	<0.001	0.72	0.36	0.85

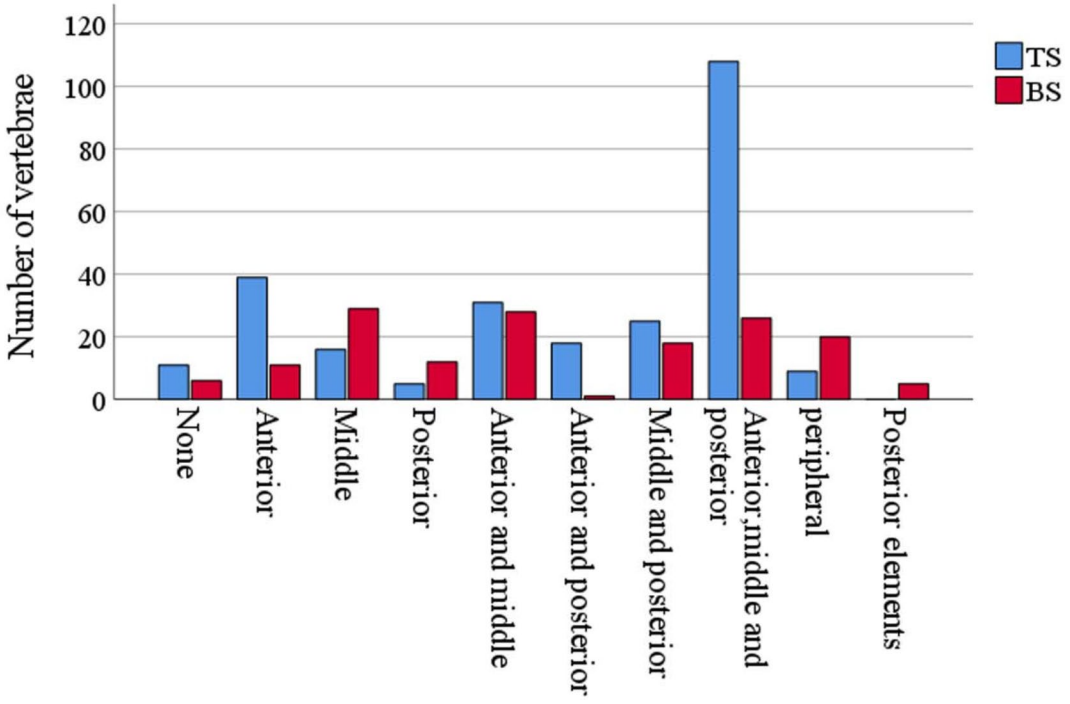

Fig. 1 Horizontal location of the erosion in patients with TS and those with BS. Extensive destruction involving each third of the vertebral body horizontally was more common in patients with TS whereas the posterior elements and peripheral area of the vertebra were destroyed more often in patients with BS($P < 0.001$). TS, tuberculous spondylitis; BS, brucellar spondylitis

(80.53% vs. 28.20%, $\chi^2 = 134.19$, $P < 0.001$, PPV = 82.75%, Figs. 2d and 3).

Although there was no statistically significant difference in sagittal or coronal osteosclerosis (9.87 vs. 11.23, $P = 0.14$ and 13.36 vs. 11.94, $P = 0.17$, respectively), more osteosclerosis was present throughout the vertebra in the TS group than in the BS group (34.73% vs. 12.82%, $\chi^2 = 24.07$, $P < 0.001$, PPV = 81.98%; Fig. 2b). By contrast, fan-shaped osteosclerosis around erosions, especially those at the anterior edge of the superior or inferior endplate, had good diagnostic value, favoring a diagnosis of BS (12.82% vs.1.15%, $\chi^2 = 71.30$, $P < 0.001$, PPV = 86.96%; Fig. 2d).

Fig. 2 Morphological presentation of osteosclerosis in patients with TS and BS. (**a** and **b**) Extensive destruction and osteosclerosis in a patient with TS. **a** Extensive destruction involved anterior, middle, and posterior thirds of the vertebra on axial image. **b** The triangular (Thick arrowhead) and rectangular (thin arrowhead) osteosclerosis spreads from the anterior wall to the posterior wall in the C3 and C4 vertebrae. (c and d) Peripheral destruction and bone formation in a patient with BS. **c** Peripheral destruction. Multiple erosions involved vertebral body except in the center and in the vertebral wall. **d** Fan-shaped osteosclerosis. The erosion (triangle) is located at the anterior edge of the endplate surrounded by sclerotic bone with a fan shape. TS, tuberculous spondylitis; BS, brucellar spondylitis

No statistically significant between-group difference was observed in the integrity of the vertebral wall (9.54% for TS vs. 20.51% for BS, $\chi^2=9.99$, $P=0.02$). However, the length and rate of destruction were significantly greater in the TS group than in the BS group (54.85 mm vs. 33.53 mm, $t=6.62$, $P<0.001$ and 47.16% vs. 23.33%, $t=8.14$, $P<0.001$, respectively). A vertebral wall destruction rate of greater than 36.40% favored a diagnosis of TS and had a PPV of 84.53%. A difference was also observed in the location of the vertebral wall destruction($\chi^2=72.38$, $P<0.001$; Fig. 4).The destruction involving the lateral portion of the vertebral wall was more common in the BS group (25.00% vs. 12.21%). Whereas, the destruction involving the anterior, lateral, and posterior walls was more common in the TS group (9.16% vs.0.64%).

The proportion of bone formation around the vertebra was greater in the BS group than in the TS group (62.18% vs. 8.40%, $\chi^2=138.89$, $P<0.001$; PPV=81.51%). The BS group showed significantly longer bone formation than the TS group (18.06 mm vs.1.97 mm, $t=14.28$, $P<0.001$). Bone formation longer than 3.00 mm around the vertebra favored a diagnosis of BS (PPV=77.66%). Anterior bone formation was longer and had a more closed morphological presentation in the BS group than in the TS group (3.86 mm vs. 0.92 mm, $t=6.51$, $P<0.001$ and 44.87% vs.

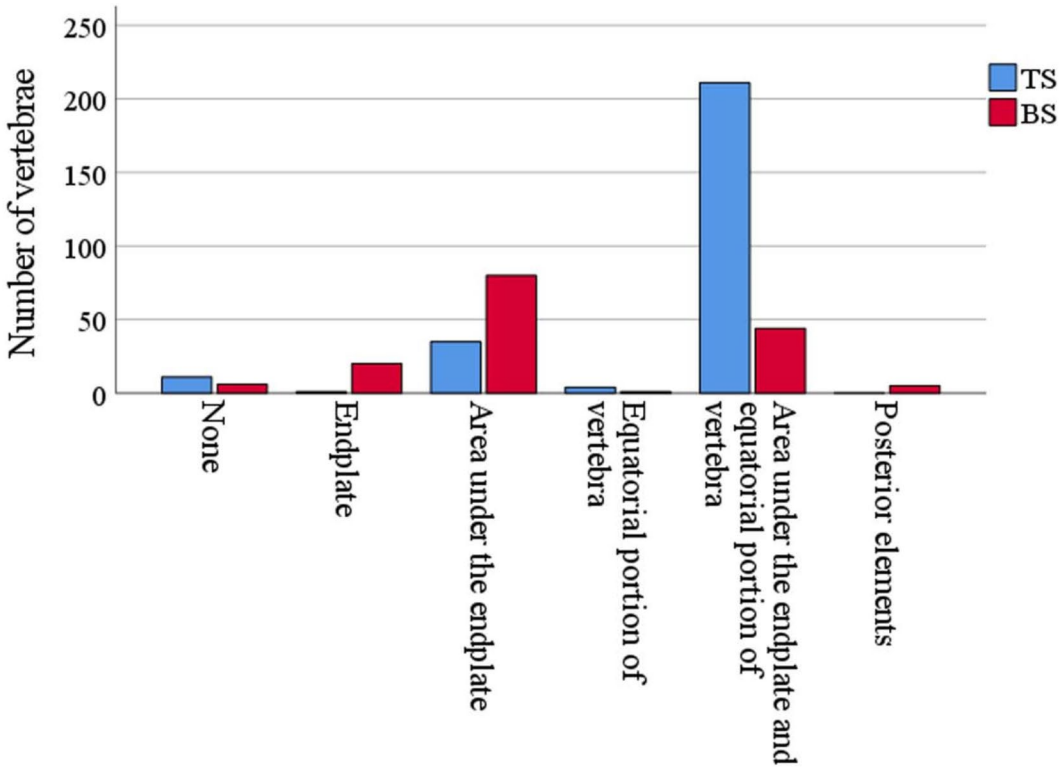

Fig. 3 Longitudinal location of the erosion in patients with TS and those with BS. The area under the endplate and the equatorial portion of the vertebra were destroyed more commonly in the TS($P<0.001$). However, the endplate and the area under the endplate were usually destroyed in BS($P<0.001$). TS, tuberculous spondylitis; BS, brucellar spondylitis

7.63%, $\chi^2=152.53$, $P<0.001$; PPV=77.78%, respectively; Fig. 5).

Sequestrum was more common in the TS group than in the BS group (45.42% vs. 3.21%, $\chi^2=83.51$, $P<0.001$, PPV=95.98%). Sequestrum was located both in and out of the erosions in the TS group, but only appeared in the erosions in the BS group. There was also a significant between-group difference in the shape and size of sequestrum; fragmented and blocked sequestrum were more common in the TS group ($\chi^2=102.43$, $P<0.001$, 22.14% vs. 0.64%, PPV=98.31% and 22.14% vs. 0.00%, PPV=100%, respectively), whereas the BS group showed only dotted and linear sequestrum (Fig. 6).

Discussion

Both TS and BS continue to be public health problems, particularly in developing countries [18]. Several studies have identified radiological features that help to distinguish different types of infectious spondylitis [11, 12, 19, 20]. However, the features of vertebral destruction cannot usually be detected clearly on MRI; they are often concealed by a hyperintense area of inflammatory edema. By contrast, CT imaging clearly reveals bone destruction and formation that have great significance in differentiating spinal infections [15].

Though duration of illness varied from patient to patient in these two spinal infections, no significant difference was found in the mean interval between presentation and CT imaging in the groups. Thus, specific changes of bony structures may mainly depend on the bacterial characteristics. Mycobacterium tuberculosis enters the vertebra through the nutrient and metaphyseal arteries with coiled terminals, remains beneath the endplate, and forms multiple TB abscesses followed by caseous necrosis [21]. Lipids in mycobacteria inhibit the activity of macrophages and lysosomes. Thus, multiple lesions cannot be absorbed, aggravate and integrate into extensive destruction, which explain the pattern of bone destruction in the TS group. Greater destruction with less bone formation results in extensive destruction involving the anterior, middle, and posterior portions of the vertebra horizontally and the areas under the endplate and the equatorial portion of the vertebra longitudinally.

The brucella organism is shorter than a mycobacterium and enters the vertebral periphery via the metaphyseal arteries and numerous tiny peripheral arteries; therefore, it can reach an area closer to the endplate than M. tuberculosis. In this study, erosions in the BS group were more commonly located in and beneath the endplate. Bone destruction in the BS group rarely involved the equatorial

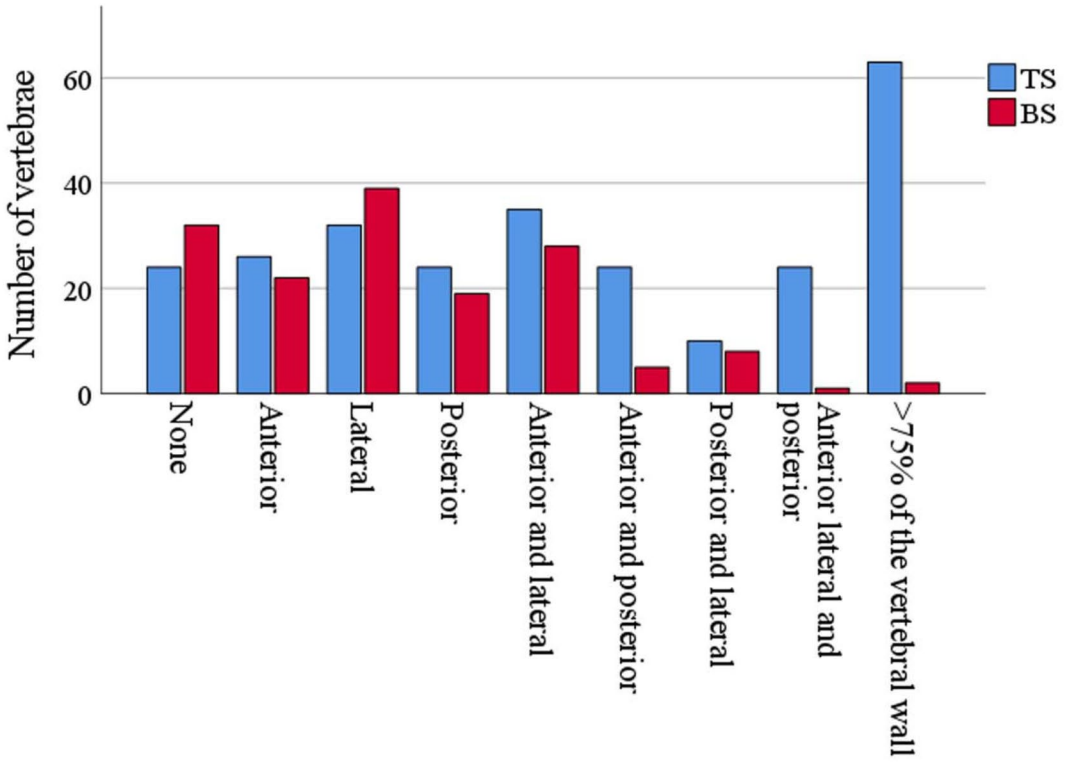

Fig. 4 Location of vertebral wall destruction in patients with TS and those with BS. The anterior, lateral, and posterior wall were destroyed more often in the TS group($P < 0.001$). Extensive destruction, defined as > 75% of vertebral wall destructed, was also commonly observed in the TS group($P < 0.001$). The lateral vertebral wall was destroyed more commonly in the BS group($P < 0.001$). TS, tuberculous spondylitis; BS, brucellar spondylitis

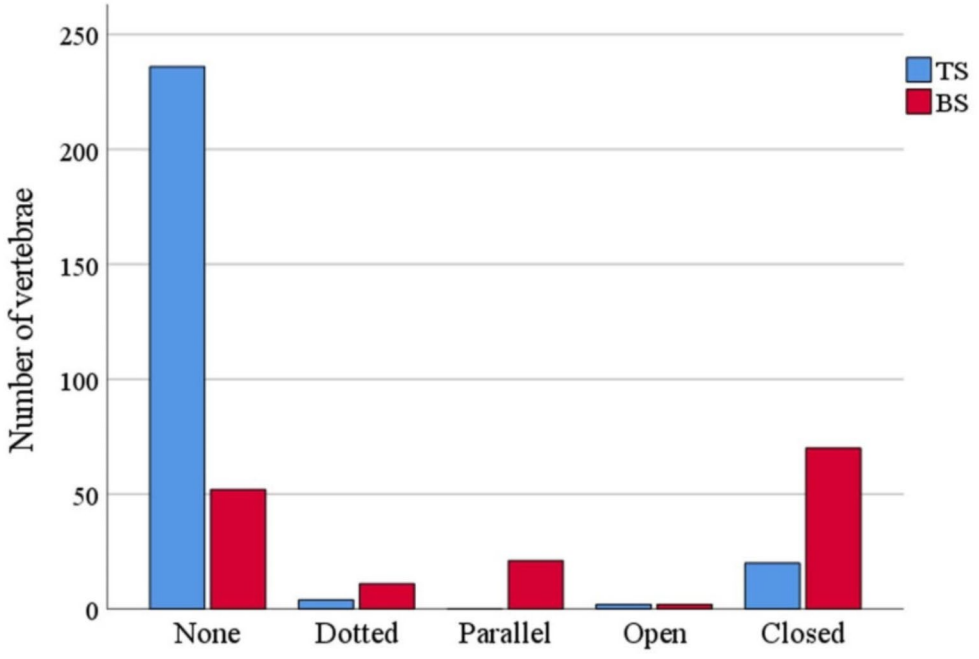

Fig. 5 Presentation of anterior bone formation in patients with TS and those with BS. The closed type of anterior bone formation was more common in the BS group than in the TS group($P < 0.001$). TS, tuberculous spondylitis; BS, brucellar spondylitis

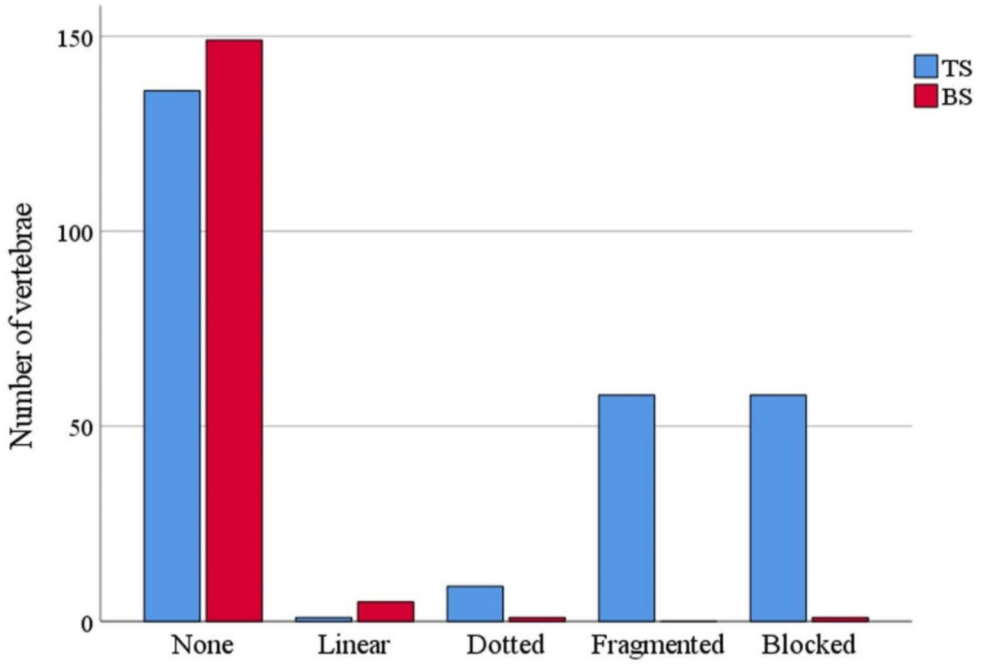

Fig. 6 Morphological presentation of sequestrum in the TS and BS groups. Fragmented and blocked sequestrum was more common in the TS group whereas the BS group showed only dotted and linear sequestrum($P < 0.001$). TS, tuberculous spondylitis; BS, brucellar spondylitis

area of the vertebra. A characteristic manifestation of BS is an isolated erosion with an osteosclerotic margin located in the anterior or posterior edge of the endplate because of its rich blood supply [12, 15]. Brucella can be easily engulfed by neutrophils and phagocytes and is less virulent than mycobacteria. This explains why bone formation was more preserved both inside and outside of the vertebra in the BS group than in the TS group.

Sequestrum is a well-recognized finding in musculoskeletal osteomyelitis [22, 23]. A tubercular lesion is difficult to absorb, leading to multiple abscesses and bone destruction with sequestration of the remaining bone, resulting in fragmented and blocked sequestrum. TS is characterized by a form of sequestrum that includes round-shaped osteolysis, peripheral bone sclerosis, and central sequestrum [24]. By contrast, brucella produces invasive and proteolytic enzymes such that sequestrum is rare. Several patients in our study showed only dotted or linear sequestrum.

This study has several limitations. The first is that cases with rare features of spondylitis may not be included because of the retrospective nature of the study and the small sample size drawn from one institution, which limit the extension of findings. The second limitation is that we excluded patients with pyogenic spondylitis, which accounts for a large share of spondylitis, which decrease the generalizability and reliability of our results. Therefore, more multicenter studies are needed to identify imaging characteristics that have high sensitivity and specificity for differentiating between all the types of spondylitis. Texture analysis, machine learning and radiomics help to quantitatively analyze bone changes and to differentially diagnose different spinal infections.

In conclusion, TS is more likely to manifest as extensive vertebral destruction with more destruction of the vertebral wall and fragmented and blocked sequestrum. By contrast, BS manifests as more isolated erosions surrounded by fan-shaped osteosclerosis, more bone formation around the vertebra, and longer anterior and closed bone formation. Changes on CT imaging may help to differentiate TS from BS and can make up for the shortcomings of other examinations. This research can further the early diagnosis and improve the cure rate in these two spinal infections.

Abbreviations

TB	Tuberculosis
TS	Tuberculous Spondylitis
BS	Brucellar Spondylitis
CT	Computed Tomography
MRI	Magnetic Resonance Imaging
STA	Standard Tube Agglutination
PPV	Positive Predictive Value
ROC curve	Receiver-Operating Characteristic curve

Author contributions

Qinpeng Xu: Conceptualization, Writing – original draft. Xingzhi Jing: Methodology, Writing – original draft. Meimei Zheng: Data collection, Software. Qinpeng Xu, Xingzhi Jing and Meimei Zheng contributed equally to this studyJianmin Sun: Statistical analysis.Xingang Cui: Methodology. Xiaoyang Liu: Conceptualization, Writing – review & editing.

Funding

The present study was supported by the National Natural Science Foundation of China (grant no. 82002325), the Natural Science Foundation of Shandong

Province (grant no. ZR2020QH075, ZR2021MH167 and ZR2023MH159) and the Municipal Innovation Plan of Clinical Medical Science and Technology of Jinan (202134043).

Data availability
The data used to support the findings of this study are included within the article.

Declarations

Ethics approval and consent to participate
Ethics approval was from the Medical Ethics Committee of Shandong Provincial Hospital Affiliated to Shandong First Medical University (SZRJJ: NO.2022 – 136). Informed consent was obtained from all study participants.

Consent for publication
All the authors read and agreed to publish this manuscript.

Competing interests
The authors declare no competing interests.

Received: 13 January 2024 / Accepted: 4 November 2024
Published online: 11 November 2024

References

1. Glaziou P, Floyd K, Raviglione MC. Global epidemiology of tuberculosis. Semin Respir Crit Care Med. 2018;39:271–85.
2. MacNeil A, Glaziou P, Sismanidis C, Maloney S, Floyd K. Global Epidemiology of Tuberculosis and progress toward achieving global targets – 2017. Morb Mortal Wkly Rep. 2019;68:263–6.
3. Polley P, Dunn R. Noncontiguous spinal tuberculosis: incidence and management. Eur Spine J. 2009;18:1096–1011.
4. Jia CG, Gao JG, Liu FS, Li Z, Dong ZL, Yao LM, et al. Efficacy, safety and prognosis of treating neurological deficits caused by spinal tuberculosis within 4 weeks' standard anti-tuberculosis treatment: a single medical center's experience. Experimental Therapeutic Med. 2020;19:519–26.
5. Franc KA, Krecek RC, Häsler BN, Arenas-Gamboa AM. Brucellosis remains a neglected disease in the developing world: a call for interdisciplinary action. BMC Public Health. 2018;18:125.
6. Turunc T, Demiroglu YZ, Uncu H, Colakoglu S, Arslan H. A comparative analysis of tuberculous, brucellar and pyogenic spontaneous spondylodiscitis patients. J Infect. 2007;55:158–63.
7. Jeong SJ, Choi SW, Youm JY, Kim HW, Ha HG, Yi JS. Microbiology and epidemiology of infectious spinal disease. J Korean Neurosurg Soc. 2014;56:21–7.
8. Yilmaz E, Parlak M, Akalin H, Heper Y, Ozakin C, Mistik R, et al. Brucellar spondylitis: review of 25 cases. J Clin Rheumatology: Practical Rep Rheumatic Musculoskelet Dis. 2004;10:300–7.
9. Arockiaraj J, Michael JS, Amritanand R, David KS, Krishnan V. The role of Xpert MTB/RIF assay in the diagnosis of tubercular spondylodiscitis. Eur Spine J. 2017;26:3162–9.
10. Frel M, Białecki J, Wieczorek J, Paluch Ł, Dąbrowska-Thing A, Walecki J. Magnetic Resonance Imaging in Differentatial diagnosis of Pyogenic Spondylodiscitis and Tuberculous Spondylodiscitis. Pol J Radiol. 2017;82:71–87.
11. Li T, Li W, Du Y, Gao M, Liu X, Wang G, et al. Discrimination of pyogenic spondylitis from brucellar spondylitis on MRI. Medicine. 2018;97:e11195.
12. Gao M, Sun J, Jiang Z, Cui X, Liu X, Wang G, et al. Comparison of tuberculous and brucellar spondylitis on magnetic resonance images. SPINE. 2017;42:113–21.
13. Zhang N, Zeng X, He L, Liu Z, Liu J, Zhang Z, et al. The Value of MR Imaging in Comparative Analysis of Spinal Infection in adults: Pyogenic Versus Tuberculous. World Neurosurg. 2019;128:e806–13.
14. Skoura E, Zumla A, Bomanji J. Imaging in tuberculosis. Int J Infect Dis. 2015;32:87–93.
15. Liu X, Zheng M, Jiang Z, Wang G, Li T, Sun J, et al. Computed tomography imaging characteristics help to differentiate pyogenic spondylitis from brucellar spondylitis. Eur Spine J. 2020;29:1490–8.
16. Liu Z, Wang J, Chen GZ, Li WW, Wu YQ, Xiao X, et al. Clinical characteristics of 1378 inpatients with spinal tuberculosis in General hospitals in South-Central China. Biomed Res Int. 2019;2019:9765253.
17. Liang C, Wei W, Liang X, De E, Zheng B. Spinal brucellosis in Hulunbuir, China, 2011–2016. Infect Drug Resist. 2019;12:1565–71.
18. Louw QA, Tawa N, Van Niekerk SM, Conradie T, Coetzee M. Spinal tuberculosis: a systematic review of case studies and development of an evidence-based clinical guidance tool for early detection. J Eval Clin Pract. 2020;26:1370–82.
19. Panta OB, Pathak YR, Karki DB. Magnetic resonance imaging findings in Spondylodiscitis. J Nepal Health Res Counc. 2018;15:217–21.
20. Foreman SC, Schwaiger BJ, Meyer B, Gersing AS, Zimmer C, Gempt J, et al. Computed tomography and Magnetic Resonance Imaging Parameters Associated with Poor Clinical Outcome in Spondylodiscitis. World Neurosurg. 2017;104:919–e9262.
21. Ali A, Musbahi O, White VLC, Montgomery AS. Spinal tuberculosis: a Literature Review. JBJS Reviews. 2019;7:e9.
22. Jennin F, Bousson V, Parlier C, Jomaah N, Khanine V, Laredo JD. Bony sequestrum: a radiologic review. Skeletal Radiol. 2011;40:963–75.
23. Shikhare SN, Singh DR, Shimpi TR, Peh WC. Tuberculous osteomyelitis and spondylodiscitis. Semin Musculoskelet Radiol. 2011;15:446–58.
24. Ousehal A, Adil A, Abdelouafi A, Kadiri R. Centrosomatic spinal tuberculosis: radiographic features in 10 cases. J Neuroradiol. 2000;27:247–52.

Publisher's note

Springer Nature remains neutral with regard to jurisdictional claims in published maps and institutional affiliations.